Received: 29 September 2021 | Revised: 16 November 2021 | Accepted: 16 November 2021

DOI: 10.1002/app.51969

ARTICLE

Applied Polymer SCIENCE WILEY

In situ monitoring of moisture uptake of flax fiber reinforced composites under humid/dry conditions

Luigi Calabrese[1] | **Vincenzo Fiore**[2] | **Elpida Piperopoulos**[1] | **Dionisio Badagliacco**[2] | **Davide Palamara**[1] | **Antonino Valenza**[2] | **Edoardo Proverbio**[1]

[1]Department of Engineering, University of Messina, Messina, Italy

[2]Department of Engineering, University of Palermo, Palermo, Italy

Correspondence
Luigi Calabrese, Department of Engineering, University of Messina, Contrada Di Dio (Sant'Agata), 98166 Messina, Italy.
Email: luigi.calabrese@unime.it

Funding information
Regione Siciliana, Grant/Award Number: G48I18001090007

Abstract

The use of green materials such as natural fiber-reinforced composites represents an increasingly stringent prerogative in the future planning of industrial and non-industrial production. The optimization of these materials is the main aim of the current research, focused on the evaluation of the behavior of flax fiber reinforced composites exposed to isothermal adsorption and desorption cycles, at varying the partial pressure of water vapor (P/P_0). For this purpose, the moisture uptake and the morphology changes of the composite material and their constituents were in situ monitored through a measurement protocol, by using a dynamic vapor sorption (DVS) analysis, coupled with an environmental scanning electron microscopy (ESEM) visual investigation. A dependence of moisture uptake and diffusivity on the composite morphology was clearly detected. In particular, no significant variation in the morphology of the specimen is noticed at low water vapor partial pressure (i.e., P/P_0 up to 5.4%) due to the limited absorption capacity (i.e., lower than 1%). On the other hand, fibers morphology changes at increasing the partial pressure up to 25.1%, showing a sensitive increase in volume. This phenomenon becomes much more relevant for high relative humidity values (i.e., ~90%), reaching more than 6% of absorption capacity.

KEYWORDS

adsorption, composites, fibers, microscopy

1 | INTRODUCTION

The continuous and wide research for advanced sustainable materials with a marked ecological footprint has led to an ever-growing interest on natural fibers reinforced composites (NFRCs).[1,2] These materials represent a promising design solution able to combine performances and environmental constrains. Natural fibers, for example, flax, jute, and sisal, are a green alternative to conventional fiberglass. The pros in the design of this class of materials is the opportunity to preserve a good compromise between strength and toughness.[3] Furthermore, cellulosic fibers are usually lightweight (i.e., low density), cheap, abundant, and sustainable (often available from

production waste).[4] This implied a growing development in ever wider engineering contexts such as the automotive,[5] aeronautics,[6,7] or construction[8,9] sectors. However, their widespread diffusion is limited by the low interfacial adhesion of the natural fibers with the polymeric matrix[10] and the wide heterogeneity of the natural raw materials which constrain their performance stability.[11] Equally relevant issue is the significant moisture absorption of natural fibers which negatively affects strength, stiffness, and adhesion with the hydrophobic matrix, accelerating the premature degradation of the composite material in wet or humid environments,[12,13]

Increasing knowledge of moisture absorption phenomena and related damage mechanisms is an important factor to ensure the design and the applicability of natural fiber-reinforced composites in industrial fields where they are randomly exposed to variable humidity conditions during their service life.[14] Moreover, these materials often operate in environments in which the moisture absorption is cyclically favored (i.e., humid or wet environments) or hindered (i.e., dry environments).

As a consequence, suitable quantitative data on water vapor diffusion phenomena in NFRCs are critical for moisture-induced damage predictions. However, these information are often incomplete due to the wide variety of environmental conditions and materials.[15]

In particular, a cyclic moisture uptake, characterized by alternate periods of exposure to wet and dry environments, leads to severe degradation of the NFRCs. These materials, due to the variation of moisture content, suffer swelling as well as shrinking during wet or dry conditions, respectively. The different behavior between the natural fiber and the polymeric matrix during the absorption and desorption steps could be the driving force to trigger NFRC mechanical degradation (e.g., matrix cracking or debonding at the fiber/matrix interface),[16,17]

Hence, the prediction of the absorption and desorption properties of the NFRCs in different environmental conditions, characterized by water vapor partial pressure variation, represents an important setting for understanding the absorption and degradation phenomena in this kind of materials.[18] In this context, the use of dynamic vapor sorption (DVS) measurements has recently proved to be an effective choice in terms of experimental affordability and scientific value of the analytical approach,[19,20,21]

However, an aspect not yet addressed in literature that the present work wants to focus on, is to evaluate how the morphological changes that take place in the composite constituents during the hydration/dehydration phases can influence the adsorption and desorption phenomena. The use of an in situ morphological analysis technique of the NFRC at varying humidity environmental conditions could be a valid tool to meet this need.

On this concern, the aim of this work is to evaluate the absorption and desorption properties of flax fiber-reinforced epoxy composites. In particular, DVS measurements were carried out in a wide relative humidity range (i.e., 0%–90% RH) on the composite material and its constituents, in order to evaluate the mechanisms and kinetics of the desorption and absorption processes. Information on the evolution of the water vapor diffusion coefficient at varying environmental conditions were acquired. Finally, an in situ monitoring of the morphological changes of flax fiber reinforced composites under humid/dry conditions was performed by using an environmental scanning electron microscopy (ESEM). This analysis was applied to evaluate the morphological changes induced by the hydration and the dehydration of the composite material in an environment with variable humidity content.

2 | EXPERIMENTAL

2.1 | Materials and methods

Square-shaped (30 cm × 30 cm × 0.335 cm) flax fibers reinforced panels were manufactured through vacuum-assisted resin infusion by using a two-stage vacuum pump model VE 235 D by Eurovacuum (Reeuwijk, The Netherlands). In particular, each panel was cured at 25°C for 24 h and post-cured at 50°C for 15 h.

A DGEBA epoxy resin (SX8 EVO by Mates Italiana s. r.l., Italy) mixed with its own amine-based hardener (100:30 by weight) and five flax twill weave woven fabrics having nominal areal weight of 318 g/m^2 (Lineo, France) were used as matrix and reinforcement of composites, respectively.

2.2 | Water vapor adsorption/desorption measurements

Water sorption isotherm tests (i.e., 30°C) on the composite laminate and their constituents (i.e., fiber and resin) were performed using a DVS analysis. In particular, a thermo-gravimetric dynamic vapor system (model DVS Vacuum by Surface Measurements Systems, UK) was used to measure the water uptake at varying the partial pressure of water vapor (P/P_0).[22,23] The water uptake is measured using a microbalance (with precision 0.1 μg) and a dynamic water vapor pressure flow control system inside the sample holder chamber. In order to avoid condensation in the chamber walls, the whole device is placed inside a temperature-controlled box. Concerning the adsorption/desorption test set-up, a conditioning step was configured. At first, the sample (i.e., ~10–20 mg and

volume ~ 8–16 mm^3) was slowly heated up to 90°C (i.e., heating rate equal to 1°C/min) and kept at this temperature for 7 h under vacuum (i.e., 10^{-1} Pa) to allow its complete drying. Then, the chamber was cooled to reach the setting temperature (i.e., 30°C) and finally an isothermal test at 30°C was performed by increasing the partial pressure of water vapor (i.e., stepwise change of P/P_0 from 0.002 to 0.9). During each P/P_0 step, the partial pressure was kept constant at the set value until the sample weight reaches the equilibrium. Finally, a reverse step with a progressive decrease of the partial pressure from 0.9 to 0.002 completed the test cycle. The absorption/desorption change in mass was calculated according to the following equation[24]:

$$w(\mathrm{g/g}) = \frac{m\left(P_{P/P_0}\right) - m_0}{m_0} \tag{1}$$

Where $m\left(P_{P/P_0}\right)$ is the equilibrium weight of the sample at the given water vapor pressure, m_0 is the weight of the dry sample.

2.3 | Estimation of the water diffusivity

The change of the water concentration with time can be obtained with the Fick's second law:

$$\frac{\partial C}{\partial t} = D\left(\frac{\partial^2 C}{\partial x^2}\right) \tag{2}$$

Where C and D are the water concentration and diffusion coefficient, respectively, x is the transport direction and t is the time. For thin films, the solution of the Fick's second law for mono-dimensional isothermal diffusion, can be expressed as:

$$\frac{M_t}{M_\infty} = 1 - \sum_{n=0}^{\infty} \frac{8}{(2n-1)^2\pi^2} \exp\left[\frac{-D(2n-1)^2\pi^2 t}{4s^2}\right] \tag{3}$$

Where M_t and M_∞ are the mass of water uptake at time t and at equilibrium, respectively, while s is the thickness of the sample. This expression, for short times, can be approximated as follows:

$$\frac{M_t}{M_\infty} = \frac{4}{s}\sqrt{\frac{Dt}{\pi}} \tag{4}$$

This equation is valid for M_t/M_∞ values up to 0.6, where a linear relationship between M_t/M_∞ and $\sqrt{t}$ is preserved.[25] Indicating with α the slope of this curve, the diffusion coefficient can be determined from Equation (4).

$$D = \alpha^2 \frac{\pi s^2}{16} \tag{5}$$

For prismatic shaped samples, an extra water uptake contribution need to be taken into account, using the correction given by Shen[26] in order to determine the real water diffusion coefficient (D_{real}):

$$D_{real} = \frac{D_{app}}{\left(1 + \frac{s}{L} + \frac{s}{w}\right)^2} \tag{6}$$

D_{app} is the water diffusion coefficient determined by Equation (5). L and W are the sample length and width, respectively. This analysis approach is quite flexible and has been applied effectively for both thermosetting resins[15] and natural fibers[27] and their composites.[28]

2.4 | In situ monitoring of water vapor uptake

ESEM analysis was carried out on flax fiber-reinforced composites, operating with an accelerating voltage of 10 kV, using isobaric conditions (i.e., 10 Pa) from 25 to 40°C, and at 40°C, in controlled water vapor atmosphere, from 10 Pa to 800 Pa (i.e., 0.1% to 10.9% of relative humidity). The sample hydration was forwarded up to 91.3% of relative humidity, dropping the temperature down to 5°C. At the end of the analysis cycle, the same conditions of dehydration (P = 10 Pa, T = 40°C) were repeated. A scheme of the analysis set-up is reported in Figure 1.

The purpose is to evaluate the morphological modification of flax fiber reinforced composites induced by the moisture uptake during a wet/dry cycle. In particular, six P/P0 steps (RH 0.1%, 5.4%, 10.9%, 25.1%, 91.3%, and 0.3%) were applied, each one with time duration 60 min. Details concerning each step are reported in Table 1.

3 | RESULTS AND DISCUSSION

3.1 | Isothermal sorption/desorption test

Dynamic water vapor sorption tests were carried out to assess the sorption isotherms of the composite laminate and their constituents (i.e., flax fiber and epoxy resin) at different water vapor partial pressures. This approach is

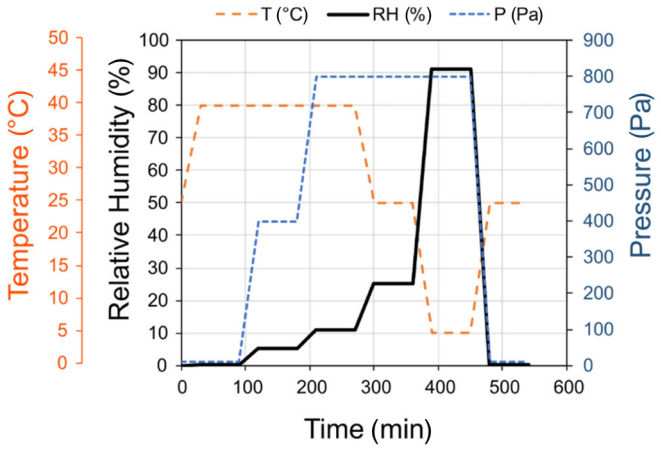

FIGURE 1 ESEM set-up for the humid/dry cycle [Color figure can be viewed at wileyonlinelibrary.com]

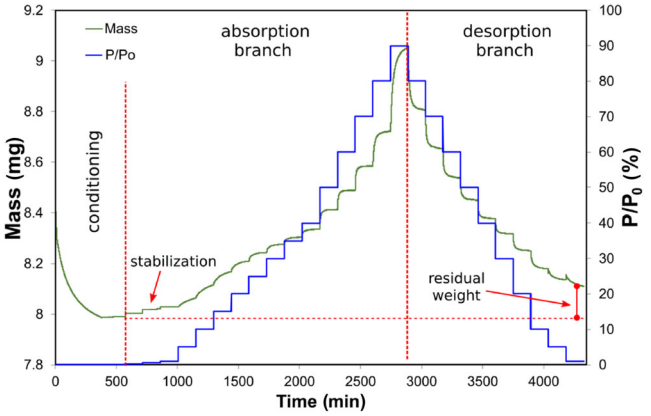

FIGURE 2 Evolution of mass change and partial pressure of water vapor (P/P_0) steps versus time during adsorption and desorption cycles for flax bundle sample [Color figure can be viewed at wileyonlinelibrary.com]

TABLE 1 Details of the experimental parameters applied during the wet/dry cycle by ESEM analysis

I	P (Pa)	T (°C)	RH (%)	Time duration
Step 0	10	25	0.3	30 min
Step 1	10	40	0.1	60 min
Step 2	400	40	5.4	60 min
Step 3	800	40	10.9	60 min
Step 4	800	25	25.1	60 min
Step 5	800	5	91.3	60 min
Step 6	10	25	0.3	60 min

suitable to assess the increase/decrease of the sample mass, up to the equilibrium, during the adsorption or desorption processes, respectively. This can be used to acquire information concerning the kinetics of the adsorption/desorption processes, thus providing an additional improvement of knowledge on their hysteresis phenomena.[29]

Figure 2 shows the evolution of the experimental change in mass as well as the partial pressure P/P_0 trend, versus time for a flax bundle sample. It can be observed that during each pressure step the mass progressively approaches a plateau value, which indicates that a saturation level was reached. Mass increase and decrease were observed for absorption and desorption branch, respectively.

As explained in the experimental section, at first, a sample conditioning at 90°C followed by cooling at 30°C under vacuum was applied to acquire a dry material. By evaluating the absorption cycle, it can be identified a stabilization phase at low P/P_0 values, where a slight mass variation occurs due to a coupled water uptake and desorption. Afterward, a rapid and gradual mass increase takes place. This effect is greater the higher the partial pressure of water vapor. Similar consideration can be argued about the desorption cycle. It is important to underline that the equilibrium value has not yet been reached at the end of the desorption cycle and the sample still exhibits a residual water content of 1.52%, due to a not complete dehydration process.[15]

The complete isothermal adsorption and desorption curves for the composite laminate and its constituents are shown in Figure 3.

This graph highlights that the isothermal sorption curve of the flax fiber exhibits a typical sigmoidal shape.[30] This curved shape is representative of cellulose-based materials and can also be generalized to many hydrophilic materials.[27] In particular, three stages can be identified,[31,32]: in the first one (i.e., stage I) at low partial pressure values (i.e., lower than 15%) the moisture content at saturation increases linearly with increasing P/P_0. During this phase, the water molecules interact with the fiber surface due to the preferential high hydrophilic sites (e.g., hydroxyl functional groups) that therefore trigger the water absorption. The second stage takes place at intermediate partial pressure values (i.e., in the range 15%–70%). In this stage, the mass variation trend is characterized by a lower slope in comparison to the first stage. In particular, the water vapor diffusion could be favored by the break of the secondary interactions, such as hydrogen bonds, between the cellulose macromolecules.[33,34] Consequently, new preferential pathways for a further permeation of water molecules are generated. The last stage, for partial pressure values higher than 70%, is characterized by a significant increase of the mass change at saturation with increasing P/P_0. This noticeable water uptake can be ascribed to the agglomeration of water

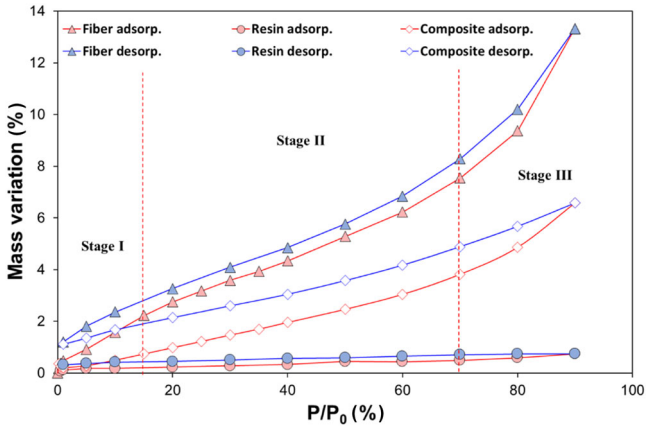

FIGURE 3 Isothermal adsorption and desorption curve at 30°C of composite and its constituents at varying the partial pressure of water vapor [Color figure can be viewed at wileyonlinelibrary.com]

molecules with the subsequent formation of clusters of absorbed water.

Quite interestingly, the adsorption and desorption curves of the flax fiber have a comparable sigmoidal shape: i.e., no relevant hysteresis is observed. This suggests the reversible nature of the process also indicating that the diffusion mechanisms that occur during the absorption and desorption steps can be considered similar. Nevertheless, Callum et al.[18] suggests that the slight differences between the adsorption and desorption cycles may be ascribed to the variation in the contact angle between the water and the internal surface of the natural fiber. In particular, the wet internal cavities of the cell wall interact with an already wet surface during the desorption cycle. Vice versa, the water film interacts with a dry surface during the adsorption cycle.

With regard the epoxy resin, it is worth noting that this polymeric material shows sorption curves almost flat, mainly due to the hydrophobic nature of the material and its intrinsically low water vapor permeability. Indeed, the mass variation is always lower than 1.0%, thus indicating the low susceptibility to water of the thermosetting polymer.

From the same plot, it is possible to note that a sigmoidal-shaped sorption isotherm, similar to that shown by flax fiber, is observed for the composite laminate. Nevertheless, some differences can be highlighted. Regardless of the partial pressure value, the water uptake is always lower than that evidenced by the flax fiber due to the presence of the hydrophobic matrix. Furthermore, in the stage III (i.e., at high P/P_0 values), the composite laminate does not exhibit a marked increase in water uptake. This behavior is attributable to the shielding effect of the epoxy matrix that hinders the rapid diffusion of the water vapor, thus limiting from a kinetic point of view the water permeation in the composite laminate. Moreover, an evident hysteresis can be identified for the composite laminate. This behavior can be ascribed to the greater difficulty of the laminate to trigger the diffusion phenomena. Furthermore, as previously highlighted, the material does not reach a clear equilibrium condition at saturation. This finding is confirmed by the presence of an adsorbed residual water at the end of desorption phase, due to the diffusion kinetic of water vapor which is the limiting factor of the process.

As already stated, the composite laminate shows a clear hysteresis due to a delay in the weight loss during the desorption branch. It is noticed that the observed desorption value is always greater than the absorption one for each P/P_0 value.

Figure 4 shows the trends of the hysteresis percentage (i.e., identified as the percentage difference between the mass variations measured during desorption and absorption branches) versus the water vapor partial pressure for the composite and its constituents. From this plot, it can be noticed that the flax fiber shows hysteresis percentage values within the range of 0.5%–1.0%. This behavior could be due to a mechanical damaging experienced by the fiber during the sorption cycle.[18] In particular, when the cell structure of the flax fiber absorbs the water vapor, it swells. More in detail, the absorbed water molecules exert pressure in the cellular structure of the fiber. When the water is desorbed, the stresses on the cell wall relax, thus leading to its shrinkage. This shrinkage is due not only to the capillary forces acting inside the cell structure of the natural fiber, but also to the presence of lignin that favors the collapse of the microcapillaries.[35]

From the same plot, it can be noticed that the hysteresis percentages shown by the epoxy resin are the lowest among the investigated samples, regardless of P/P_0 values. This finding is due to the very low sorption capacity of the thermosetting resin.

On the other hand, it is important to underline that the composite sample presents significantly higher hysteresis values than those shown by each constituent (i.e., fiber and resin). This behavior can be ascribed to the synergistic action of the absorption and desorption phenomena (such as structural swelling and capillary condensation) that take place on the constituents, which influence the sorption capacity of the composite laminate.[36] The natural fiber, embedded in the thermoset matrix, is constrained in mobility. Consequently, the fiber-matrix interface plays an important role in the stress distribution due to swelling and relaxation phenomena that occur during the absorption and desorption phases, respectively. The consequence is an amplification of the sorption hysteresis. Furthermore, water vapor mass diffusion phenomena at the fiber-matrix

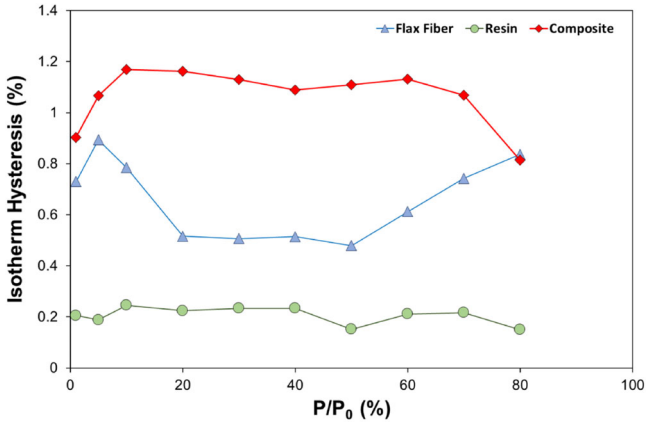

FIGURE 4 Isothermal hysteresis at 30°C of composite and its constituents at varying the partial pressure of water vapor [Color figure can be viewed at wileyonlinelibrary.com]

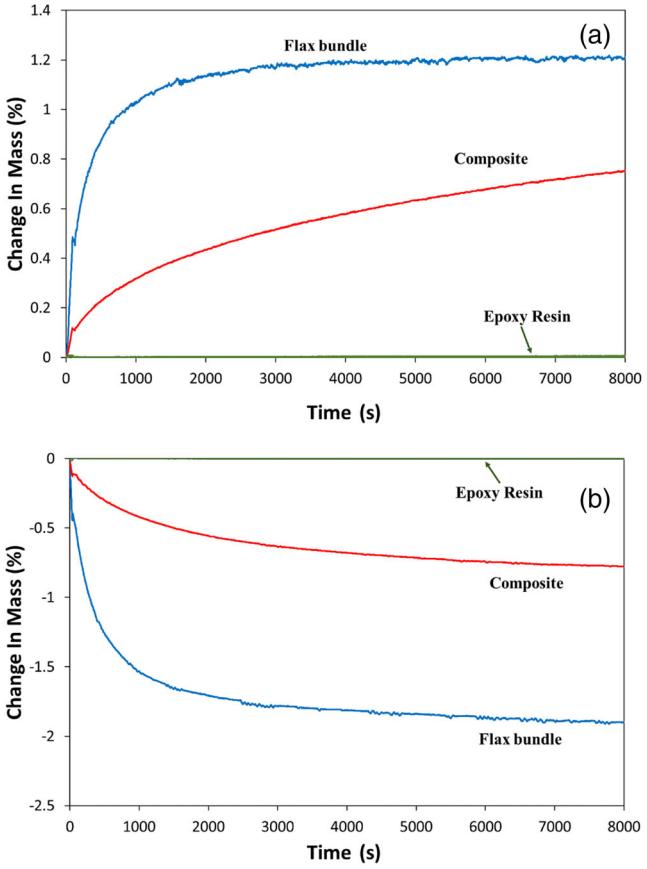

FIGURE 5 Change in weight of composite and its constituents during pressure drop at $P/P_0 = 0.7$ in (a) absorption and (b) desorption steps [Color figure can be viewed at wileyonlinelibrary.com]

interface can take place during the hydration and dehydration phases. These can influence the sorption process for capillary condensation and the related kinetic mass diffusion issues.

In order to have further insights on this behavior, Figure 5 compares the weight change of neat resin, flax fiber, and composite during pressure drop in the partial pressure step at $P/P_0 = 0.7$ during absorption (Figure 5a) and desorption (Figure 5b) branches. The mass variation when the pressure step is applied is considered as origin of the measurement. The epoxy resin does not show a significant mass change in both steps (i.e., the green curve is almost parallel to *x*-axis), confirming the low water permeability of the thermoset material.[15]

It is worth noting that the change in mass, due to water sorption, is always significantly faster for flax fiber bundles than the composite. The fibers reach a plateau both in the absorption and desorption steps in about 2000 s. Vice versa, the composite showed a monotone curve with a progressive increase (for absorption step in Figure 5a) without reaching a stabilization up to 8000 s. The water uptake, at the end of the absorption step at P/P_0 equal to 0.7, is more relevant for flax fibers (i.e., 1.19%) compared to the composite laminate (i.e., 0.75%). A similar behavior can be found during the desorption step (Figure 5b). However, in this step the mass change experienced by the flax bundles at equilibrium is equal to −1.89%, significantly lower than that of the absorption one (i.e., 1.19%).

Furthermore, it can be noticed that the composite has a faster desorption kinetic, reaching a plateau in the mass change equal to −0.77% at about 6000 s. This value is almost similar to that evidenced during the absorption step.

This behavior can be ascribed to the hydrophobic nature of the epoxy matrix that absorbs almost near to zero water content during both steps. The higher lower affinity of the epoxy matrix to water in comparison to the natural fiber implies two effects on the composite. The first one consists in the shielding effect of the matrix. It reduces the water diffusion capacity of the composite, also preventing swelling and shrinking of the fiber that represents the hydrophilic constituent of the composite laminate. At the same time, the long residence time of the water (i.e., also after drying cycles) can favor softening phenomena.[37]

The diffusion coefficient values both for the composite and the flax fiber at varying the water vapor partial pressure are reported in Figure 6. Due to the low sorption capacity of the epoxy resin, the related data are not included in the plot.

By observing this graph, it is evident that D depends appreciably on the water partial pressure. In particular, a progressive raise of the diffusion coefficient of the flax fiber can be noticed when a humidity increase is observed, starting from dry condition. A maximum is reached at intermediate humidity range (40%–70% RH).

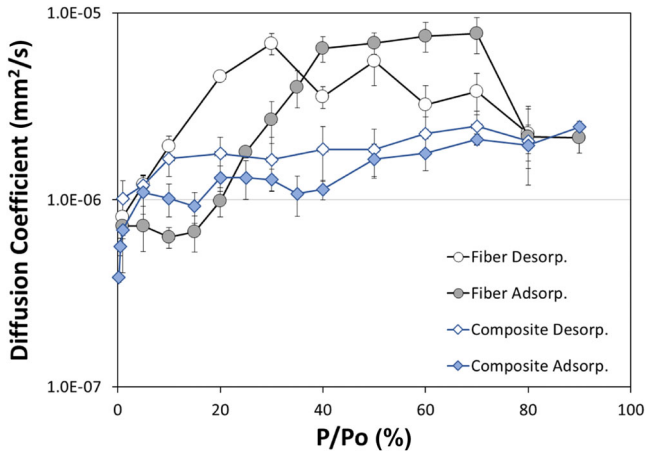

FIGURE 6 Diffusion coefficient trend versus partial pressure of water vapor at 30°C for flax bundle and composite [Color figure can be viewed at wileyonlinelibrary.com]

Afterward, a decrease of D values for higher partial pressure takes place. Similar trend is also reported in the literature for analogous natural fibers and composites.[38,39]

This initial trend at low P/P_0 values is caused by the plasticization of the material (i.e., increase of the free volume) that favors the mass diffusion phenomena.[27] At the same time, the decrease of the diffusion coefficient found for higher water vapor partial pressure can be mainly ascribed to the water molecules clustering that forms aggregates.[30]

Furthermore, the comparison between the flax bundle and composite clearly shows that the water diffusion coefficient decreases of about half decade for the NFRC than the flax bundle.

This finding suggests the presence of a shielding barrier over the fiber surface, represented by the thermosetting resin that embeds the fibers, thus limiting the diffusion process.

As concern the composite, a gradual increase of the diffusion coefficient can be noticed at increasing the partial pressure. This behavior could be associated with the capillary condensation phenomena which take place at high water vapor partial pressure and which contribute to the diffusion kinetics of water at the fiber-matrix interface in the composite material.

The D values observed for the flax fiber and the composite vary around 4.6×10^{-6} mm^2/s and 1.8×10^{-6} mm^2/s, respectively. These data are in accordance to other literature results on similar experimental tests of flax based composite laminates.[30,40]

Furthermore, noticeable differences are found by comparing the trend of the diffusion coefficient in the absorption and desorption phases. Concerning the flax fiber bundle, D is high (i.e., 7.8×10^{-6} mm^2/s) during the adsorption phase at high P/P_0 values. Vice versa, it can be noticed that the diffusion of water vapor is kinetically favored during the desorption phase for low P/P_0 values (i.e., the highest value equal to 6.9×10^{-6} mm^2/s is reached at 30% RH). The transition occurs at about 40% RH, mainly due to a significant decrease of the diffusion coefficient in the adsorption phase for low partial pressure values. On the other hand, the D value during the desorption phase remains relatively constant by reducing the partial pressure (i.e., average value equal to 1.8×10^{-6} mm^2/s in 30%–90% RH range).

The results about the kinetics of water vapor diffusion in the composite clearly suggest that even if the fibers are embedded in the thermosetting resin, which offers a shielding effect, mass diffusion phenomena remain relevant. Local hydrophilic fiber exposure as well as surface defects and fiber-matrix interface are active sites in diffusion phenomena, thus indicating that this issue remains relevant for this class of materials in the whole water vapor partial pressure range.

3.2 | In situ monitoring of water vapor uptake

In order to assess both the morphology changes of the natural fiber and its interaction with the epoxy matrix during the absorption and desorption phases, and in situ monitoring of the morphological evolution of the composite was carried out both in a wet and dry environment. For this purpose, an environmental electron scanning microscopy analysis was used applying a whole humidity cycle in a composite sample.

Figure 7 shows the bending fracture surfaces of the composite at different values of the water vapor partial pressure. In particular, Figure 7a, referring to the specimen in the dry state (i.e., RH = 0.1%), shows the surface fracture portion in which a fiber pull-out occurred. In more detail, this figure evidences the irregular geometry of the natural fibers, having diameter in the range 15–28 μm. At the same time, they present irregular roughness in addition to noticeable variability in the cross-section dimension (Point 4 in Figure 7a). Furthermore, Points 1 and 2 evidence some local discontinuities in correspondence of the fiber-matrix interface. This suggests a weak adhesion between flax fibers and the surrounding epoxy matrix. Point 3 also indicates the presence of small defects and rivers in the matrix, related to the crack propagation in the thermosetting matrix.

Figure 7b shows the fractured surface of the composite in wet condition (i.e., exposed for 1 h at 91.3% RH). Overall, these images evidence clear differences between the morphologies of the composite under dry and wet

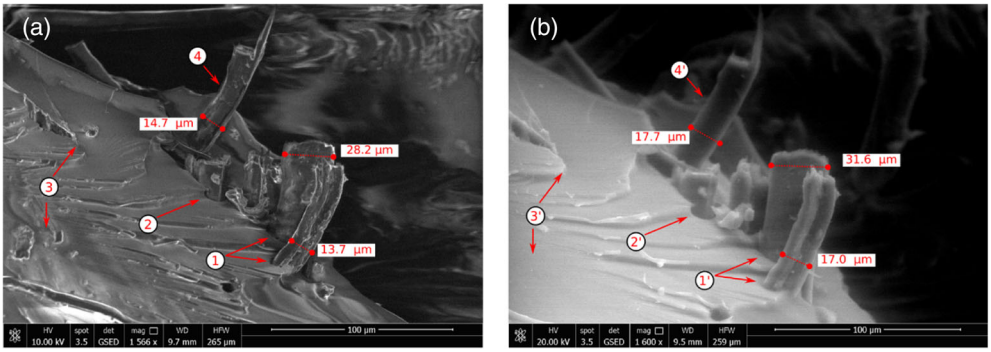

FIGURE 7 SEM micrographs of composite fracture surfaces under (a) dry (RH 0.1%) and (b) wet (RH 91.3%) conditions [Color figure can be viewed at wileyonlinelibrary.com]

conditions. At first, the diameter of flax fibers significantly increases, due to the swelling phenomenon induced by the water vapor absorption. In particular, the thin fibers (i.e., diameter ~ 15 µm) show a diameter increase of about 20% after the exposition to the wet environment. Conversely, larger fibers (i.e., diameter ~ 28 µm) exhibit a variation in their diameter of about 12%. These different increments are attributable to the fibrils distribution in the microstructure of the fiber, which constitute a rigid skeleton that hinders the volume expansion induced by the water absorption.Furthermore, fibers have a smoother and more regular surface after the composite exposition to the wet environment. Indeed, Point 4′, referred to a local thin cross-section, shows a natural fiber with an almost smoot and regular shape.

Further interesting considerations can be drawn by analyzing the fiber-matrix interface areas (Points 1′ and 2′). Due to the highly relevant swelling phenomenon for the hydrophilic fiber in comparison to the hydrophobic matrix, a better interlocking between the fiber and the matrix can be highlighted. In particular, Point 1′ shows that the fiber/matrix interfacial discontinuity disappears. This is due to the natural fiber expansion confined within the rigid matrix channel. However, in Point 2′, referred to a more irregular interfacial area, the diameter increase of the fiber is not sufficient to compensate the mismatch between fiber and matrix in the dry phase (Point 2). Consequently, a slight irregular interface remains even at the end of the hydration cycle at 91.3% of RH. Therefore, the differential expansion in wet state between fiber and matrix plays a key role on the interfacial properties of the composite, thus affecting both the absorption and laminate performance in aged conditions.[41,42] The matrix also absorbs water vapor and undergoes a surface swelling as evidenced by the smoother and more regular surface (i.e., Point 3′ in Figure 7b) than dry one (i.e., Point 3 in Figure 7a).

Figure 8 is proposed to better relate the dynamic vapor measurements with the in situ morphological investigation carried out by ESEM. In particular, the isothermal absorption curve for the flax fiber bundle is related with the

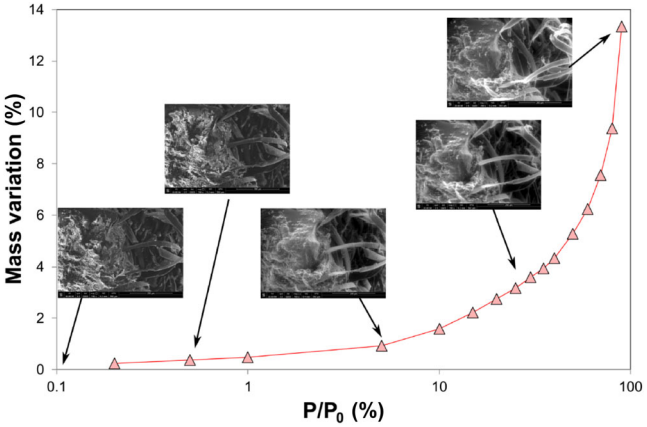

FIGURE 8 In situ monitoring of composite morphology and isothermal adsorption curve at 30°C for flax fiber bundle at varying the partial pressure of water vapor [Color figure can be viewed at wileyonlinelibrary.com]

morphological changes induced on the composite by the progressive absorption of water vapor. From this graph, it is possible to notice that no significant variation in the surface morphology occurs for partial pressure values up to 5.4%. On the other hand, the specimen surface shows a noticeable increase in the volume of flax fibers at intermediate partial pressure values (i.e., 25.1%), due to their relevant hydrophilic behavior and high absorption capability. This phenomenon becomes much more relevant for high relative humidity values, as confirmed by the exponential increase of the mass variation for high P/P_0 values (see in Figure 8 the SEM image at 91.3% RH).

Figure 9 relates the mass variation of the absorption versus swelling curve at the different analyzed partial pressures. The swelling index of the natural fiber was calculated as $100 \cdot (d_i - d_0)/d_0$. Where d_0 and d_i are the fiber diameter in dry and in ith water vapor partial pressure conditions, respectively. By this way, the swelling can be calculated at increasing P/P_0 values, using information shown in Figure 8.

Consequently, Figure 9 has the aim to quantify the correlation between swelling and variation in mass

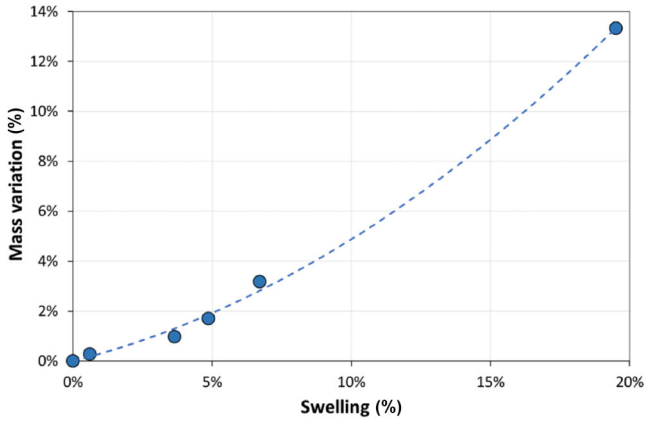

FIGURE 9 Mass variation versus swelling curve of flax bundle sample during isothermal adsorption step at different P/P_0 values [Color figure can be viewed at wileyonlinelibrary.com]

during the absorption of water vapor. There is a monotonous increase in mass absorption as the swelling varies, confirming that a common physical process (water vapor absorption) originates these phenomena. There is no linear correlation between these parameters. The sorption mass variation increases significantly at increasing swelling. This is justifiable considering that the swelling is a linear parameter, while the mass variation is a volumetric parameter. By analyzing Figure 9, it can be, furthermore, observed that the geometric variation of the fiber becomes relevant already at low water vapor absorption values. The 2% water absorption implies a cross-section variation of the fiber of 5%, sufficient to influence the interference of the fiber inside the rigid resin cavity in which it is embedded.

This confirms that the adsorption and the release of water vapor in NFRCs is associated with diffusion phenomena in their constituents at the interface. Flax fibers are interesting and promising materials in NFRC design. However, the present results confirm that it is necessary to pay attention to a limited durability in humid or wet environments due to differential swelling or shrinkage phenomena between the composite constituents, which can affect its long-term stability. Potentially, even short exposure cycles in a humid environment can leave permanent consequences in the composite even at the end of a long drying period. Certainly, a future development, aimed to better relate the absorption and desorption phenomena of water vapor to variable wet-dry cycles and how these affect the residual properties of the composite, is a good refining approach able to have a further improvement of knowledge in this research context. Further studies could be addressed in order to minimize the degradation issues that occur during aging in wet/humid environments on natural fiber composites. In this case, a potentially effective strategy can be represented by tailoring the surface properties of the fiber, for example, by means of surface treatments, in order to increase hydrophobicity and limit swelling phenomena.

4 | CONCLUSION

The main aim of the present paper is to investigate the absorption and desorption properties of flax fiber-reinforced epoxy composites. To this scope, DVS measurements were performed in a wide range of relative humidity (i.e., 0%–90% RH) on the composite material and its constituents, thus evaluating the mechanisms and kinetics of the desorption and the absorption processes. Furthermore, an in situ monitoring of the morphological changes of the composite under humid/dry conditions was performed by using an ESEM.

The experimental results allowed to reveal important findings and to draw interesting conclusions. In particular:

- A dependence of moisture uptake and diffusivity on the composite morphology was clearly detected. The composite material evidenced an intermediate trend between its constituents (i.e., the hydrophobic epoxy matrix and the hydrophilic flax fibers), showing a maximum in the water absorption of about 6%.
- The hysteresis shown by the flax fiber during the desorption phase, became more accentuated for the composite material. This characteristic can be ascribed to the synergistic action of structural swelling and capillary condensation, which occur on the constituents and consequently influence the absorption and desorption capacity of the laminate.
- The ESEM investigation highlighted greater swelling for thinner flax fibers (i.e., 20%) than for thicker ones (i.e., 12%). Specifically, the great swelling was experienced only at high relative humidity values (i.e., ~90%), coupled with a noticeable variation in the composite mass mainly due to high water absorption of flax fibers (~14%). On the other hand, the matrix was mainly subjected to a superficial swelling, which played a fundamental role especially at the interface with the fiber.

Overall, this survey protocol allowed to better understand the behavior of natural fiber-reinforced composites under humid/dry conditions in order to optimize their performances and better use them in large-scale applications, thus transforming them into consolidated structural materials.

ACKNOWLEDGMENTS

This research follows from Project "SI-MARE – Soluzioni Innovative per Mezzi navali ad Alto Risparmio Energetico"

(P.O. FESR Sicilia 2014/2020) code 08ME7219090182 - CUP G48I18001090007. Open access Funding provided by Universita degli Studi di Messina within the CRUI-CARE Agreement.

DATA AVAILABILITY STATEMENT

Research data are not shared.

ORCID

Luigi Calabrese https://orcid.org/0000-0002-2923-7664
Vincenzo Fiore https://orcid.org/0000-0002-9794-1362
Elpida Piperopoulos https://orcid.org/0000-0001-7960-4234
Dionisio Badagliacco https://orcid.org/0000-0001-9464-2853
Davide Palamara https://orcid.org/0000-0002-3806-6449
Antonino Valenza https://orcid.org/0000-0002-3236-3565
Edoardo Proverbio https://orcid.org/0000-0002-6679-7214

REFERENCES

[1] S. Sathish, N. Karthi, L. Prabhu, S. Gokulkumar, D. Balaji, N. Vigneshkumar, T. S. Ajeem Farhan, A. AkilKumar, V. P. Dinesh, *Mater. Today Proc.* **2021**, *45*, 8017.
[2] L. Kerni, S. Singh, A. Patnaik, N. Kumar, *Mater. Today Proc.* **2020**, *28*, 1616.
[3] Y. Wu, C. Xia, L. Cai, A. C. Garcia, S. Q. Shi, *J. Clean. Prod.* **2018**, *184*, 92.
[4] A. A. M. Moshi, D. Ravindran, S. Bharathi, V. Suganthan, G. K. S. Singh, *IOP Conf. Ser. Mater. Sci. Eng.* **2019**, *574*, 012013.
[5] M. Noryani, S. M. Sapuan, M. T. Mastura, M. Y. M. Zuhri, E. S. Zainudin, *IOP Conf. Ser. Mater. Sci. Eng.* **2018**, *368*, 012002.
[6] F. Jahan, M. Soni, *Mater. Today Proc* **2021**, *46*, 6708.
[7] M. Jawaid, M. Thariq, *Sustainable Composites for Aerospace Applications*, Elsevier, Kidlington, UK **2018**, p. 253.
[8] J. Claramunt, L. J. Fernández-Carrasco, H. Ventura, M. Ardanuy, *Constr. Build. Mater.* **2016**, *115*, 230.
[9] K. T. Lau, P. Y. Hung, M. H. Zhu, D. Hui, *Compos. Part B Eng.* **2018**, *136*, 222.
[10] C. H. Lee, A. Khalina, S. H. Lee, *Polymers (Basel).* **2021**, *13*, 438.
[11] F. Chegdani, M. El Mansori, S. Mezghani, A. Montagne, *Compos. Sci. Technol.* **2017**, *150*, 87.
[12] L. Calabrese, V. Fiore, T. Scalici, A. Valenza, *J. Appl. Polym. Sci.* **2019**, *136*, 47203.
[13] V. Fiore, C. Sanfilippo, L. Calabrese, *Polymers (Basel).* **2020**, *12*, 716.
[14] V. Fiore, L. Calabrese, T. Scalici, A. Valenza, *Compos. Part B Eng.* **2020**, *187*, 107864.
[15] K. M. B. Jansen, M. F. Zhang, L. J. Ernst, D. K. Vu, L. Weiss, *Microelectron. Reliab.* **2020**, *107*, 113596.
[16] A. Le Duigou, P. Davies, C. Baley, *Polym. Degrad. Stab.* **2009**, *94*, 1151.
[17] M. M. Thwe, K. Liao, *Compos. Sci. Technol.* **2003**, *63*, 375.
[18] C. A. S. Hill, A. Norton, G. Newman, *J. Appl. Polym. Sci.* **2009**, *112*, 1524.
[19] X. Zhang, J. Li, Y. Yu, H. Wang, *J. Mater. Sci.* **2018**, *53*, 8241.
[20] Q. Chen, G. Wang, X. X. Ma, M. L. Chen, C. H. Fang, B. H. Fei, *Ind. Crop. Prod.* **2020**, *151*, 112467.
[21] J. Yuan, Q. Chen, B. Fei, *Eur. J. Wood Wood Prod.* **2021**, *79*, 1131.
[22] L. Calabrese, L. Bonaccorsi, A. Freni, E. Proverbio, *Appl. Therm. Eng.* **2017**, *124*, 1312.
[23] N. Volkova, V. Ibrahim, R. Hatti-Kaul, L. Wadsö, *Carbohydr. Polym.* **1817**, *2012*, 87.
[24] L. Calabrese, L. Bonaccorsi, P. Bruzzaniti, A. Frazzica, A. Freni, E. Proverbio, *Energy* **2018**, *7*, 1.
[25] F. Badii, W. MacNaughtan, J. R. Mitchell, I. A. Farhat, *Chem. Biochem. Eng. Q.* **2013**, *32*, 30.
[26] C.-H. Shen, G. S. Springer, *J. Compos. Mater.* **1976**, *10*, 2.
[27] S. Alix, E. Philippe, A. Bessadok, L. Lebrun, C. Morvan, S. Marais, *Bioresour. Technol.* **2009**, *100*, 4742.
[28] D. Jain, I. Kamboj, T. K. Bera, A. S. Kang, R. K. Singla, *Int. J. Heat Mass Transf.* **2019**, *130*, 431.
[29] C. A. S. Hill, A. Norton, G. Newman, *J. Appl. Polym. Sci.* **2010**, *116*, 2166.
[30] F. Gouanvé, S. Marais, A. Bessadok, D. Langevin, M. Métayer, *Eur. Polym. J.* **2007**, *43*, 586.
[31] A. Bessadok, S. Marais, F. Gouanvé, L. Colasse, I. Zimmerlin, S. Roudesli, M. Métayer, *Compos. Sci. Technol.* **2007**, *67*, 685.
[32] Z. El Hachem, A. Célino, G. Challita, M. J. Moya, S. Fréour, *Ind. Crop. Prod.* **2019**, *140*, 111634.
[33] A. Sharma, S. Thakre, G. Kumaraswamy, *Cellulose* **2020**, *27*, 1195.
[34] B. Lindman, B. Medronho, L. Alves, C. Costa, H. Edlund, M. Norgren, *Phys. Chem. Chem. Phys.* **2017**, *19*, 23704.
[35] A. N. Papadopoulos, *Holz Roh Werkst.* **2005**, *63*, 437.
[36] Y. Xie, C. A. S. Hill, Z. Jalaludin, D. Sun, *Cell* **2011**, *18*, 517.
[37] T. Cadu, L. Van Schoors, O. Sicot, S. Moscardelli, L. Divet, S. Fontaine, *Ind. Crop. Prod.* **2019**, *141*, 111730.
[38] F. Gouanvé, S. Marais, A. Bessadok, D. Langevin, C. Morvan, M. Métayer, *J. Appl. Polym. Sci.* **2006**, *101*, 4281.
[39] A. Murr, *Transp. Porous Media* **2019**, *128*, 385.
[40] A. Arbelaiz, B. Fernández, J. A. Ramos, A. Retegi, R. Llano-Ponte, I. Mondragon, *Compos. Sci. Technol.* **2005**, *65*, 1582.
[41] D. E. C. Depuydt, J. Soete, Y. D. Asfaw, M. Wevers, J. Ivens, A. W. van Vuure, *Compos. Part A Appl. Sci. Manuf.* **2019**, *119*, 48.
[42] H. N. Dhakal, Z. Y. Zhang, M. O. W. Richardson, *Compos. Sci. Technol.* **2007**, *67*, 1674.

How to cite this article: L. Calabrese, V. Fiore, E. Piperopoulos, D. Badagliacco, D. Palamara, A. Valenza, E. Proverbio, *J. Appl. Polym. Sci.* **2022**, *139*(16), e51969. https://doi.org/10.1002/app.51969